crystals

MDPI

Article

Exploring the Wet Mechanochemical Synthesis of Mg-Al, Ca-Al, Zn-Al and Cu-Al Layered Double Hydroxides from Oxides, Hydroxides and Basic Carbonates

Brenda Antoinette Barnard * and Frederick Johannes Willem Jacobus Labuschagné

Department of Chemical Engineering, University of Pretoria, Lynnwood Rd, Hatfield, Pretoria 0002, South Africa; johan.labuschagne@up.ac.za

* Correspondence: u14037948@tuks.co.za

Received: 21 September 2020; Accepted: 16 October 2020; Published: 20 October 2020

Abstract: The synthesis of Mg-Al, Ca-Al, Zn-Al and Cu-Al layered double hydroxides (LDHs) was investigated with a one-step wet mechanochemical route. The research aims to expand on the mechanochemical synthesis of LDH using a mill designed for wet grinding application. A 10% slurry of solids was added to a Netzsch LME 1 horizontal bead mill and milled for 1 h at 2000 rpm. Milling conditions were selected according to machine limitations and as an initial exploratory starting point. Precursor materials selected consisted of a mixture of oxides, hydroxides and basic carbonates. Samples obtained were divided such that half was filtered and dried at 60 °C for 12 h. The remaining half of the samples were further subjected to ageing at 80 °C for 24 h as a possible second step to the synthesis procedure. Synthesis conditions, such as selected precursor materials and the M^{II}:M^{III} ratio, were adapted from existing mechanochemical methods. LDH synthesis prior to ageing was successful with precursor materials observably present within each sample. No Cu-Al LDH was clearly identifiable. Ageing of samples resulted in an increase in the conversion of raw materials to LDH product. The research offers a promising 'green' method for LDH synthesis without the production of environmentally harmful salt effluent. The synthesis technique warrants further exploration with potential for future commercial up-scaling.

Keywords: layered double hydroxide; mechanochemistry; bead mill; green chemistry; synthesis; wet grinding

1. Introduction

Layered double hydroxides (LDHs) are clay-like minerals commonly referred to as anionic clays with a wide range of physical and chemical properties. They are represented by the general formula $[M^{II}_{1-x}M^{III}_{x}(OH)_2][X^{q-}_{x/q}\cdot H_2O]$ in which M^{II} and M^{III} represent the selected divalent and trivalent metal elements and $[X^{q-}_{x/q}\cdot H_2O]$ denotes the interlayer composition. LDHs often find application in pharmaceuticals, as polymer additives, as additives in cosmetics, and in catalysis. This is due to having variable layer charge density, reactive interlayer space, ion exchange capabilities, a wide range of chemical compositions and rheological properties [1]. LDH materials can be synthesised using various different techniques of which the most common are co-precipitation, reconstruction, hydrothermal methods and urea decomposition-homogenous precipitation. The primary principle associated with these methods include the precipitation of various types of metal ions which makes large scale production difficult. Challenges associated with these methods include differing precipitation rates of metal ions, need for inert environments, production of environmentally harmful waste and high production costs [2]. Novel, 'green' synthesis techniques are therefore often sought

after. Recently the use of mechanochemistry as an alternative synthesis procedure has gained wide-spread attention. Mechanochemistry is considered a versatile method of synthesis with the promise of producing LDH materials with unique elemental combinations [3,4]. The most common types of mechanochemical synthesis techniques include single-step or one-pot grinding [5,6], mechano-hydrothermal synthesis [7–10] and two step grinding. Two-step grinding can consist of an initial grinding step followed by an additional treatment step or a second grinding step [11–13]. Grinding of raw materials can be conducted wet, dry or as a paste. Various techniques and combinations involving the wet or dry milling of raw materials have been attempted and found to be successful [2]. Studies have shown that the type of grinding technique can largely affect the success of LDH synthesis, with some techniques not producing sufficient mechanical energy for the synthesis to occur readily [11]. Research has indicated that a large amount of mechanochemical methods explored typically involve the use of ball mills, mixer mills or a mortar and pestle as the primary grinding technique [2]. The final properties of LDH are further influenced by the selected method of grinding [14]. It is therefore of interest to expand on the effect of milling techniques on the synthesis of LDH materials. The success associated with the formation of an LDH phase for single step grinding procedures are further influenced by the selected starting materials [2]. The use of metallic salts of chlorides or nitrates allows for LDH synthesis but introduces a washing step that could produce an undesirable waste solution [5,6]. The use of hydroxides and oxides eliminates the production of waste solution promoting 'green' synthesis of LDH materials, however, has proven to be challenging [2]. The addition of water to existing grinding techniques, such that wet grinding occurs, is considered unsuitable for solid state chemistry as it may reduce the degree of amorphitization and prevent active site formation [15]. Dry grinding is therefore typically conducted as an initial mechanochemical step when synthesising LDHs. The absence of water allows for sufficient active site formation and amorphitisation. Dry grinding of the precursor materials is regularly used in conjunction with a second synthesis step. A variation of secondary synthesis steps have been explored. LDH materials have successfully been synthesised with the dry grinding of raw materials and agitating the milled material in a solution containing the desired anion for intercalation [16–19]. Similarly, LDH synthesis methods have involved dry grinding followed by washing or thermal treatment of the sample [2,20]. Unique methods have also involved a combination of the initial dry grinding step with that of a wet grinding step [15,21] or methods involving ultrasonic irradiation [22–24]. Limited research has been conducted on single-step or one-pot wet grinding and low conversion rates obtained warrant the need for further research [2,25]. Incomplete conversion or no LDH formation have been attributed to the quantity of water present with insufficient mechanochemical activation of the precursor materials occurring [15]. The study therefore aims to expand on the one-step wet mechanochemical synthesis of layered double hydroxides, from oxides, hydroxides and basic carbonates, by making use of a Netzsch LME 1 horizontal bead mill. The selected mill is designed specifically for wet grinding application and allows for the continuous, semi batch or batch synthesis of LDH materials. The process could be easily up scaled to produce large volumes of consistent and commercially viable LDH product. Precursor materials and M^{II}:M^{III} ratios were adapted from mechanochemical techniques in which LDH synthesis was successful [15,17,18,21]. The performance of the selected mill and synthesis conditions could therefore be investigated. Samples obtained were further subjected to ageing at 80 °C to determine the effects of including a thermal step to the selected mechanochemical method.

2. Materials and Methods

2.1. Milling Operation

Selected raw materials were wet batch milled with the use of a Netzsch LME 1 horizontal bead mill, under air atmosphere. The milling chamber (1.225 L) was loaded to a capacity of 60% (by volume) with 2 mm diameter yttrium stabilised zirconia beads. Cooling water was allowed to circulate through the outer jacket of the milling chamber at a constant inlet temperature of 30 °C and flow rate of

525 L·h^{-1}. A water slurry consisting of 10% solids (reactants) was added to the milling chamber and milled for 1 h at 2000 rpm. Samples obtained were divided such that half was filtered and dried at 60 °C for 12 h. The remaining half of the sample was subjected to ageing at 80 °C for 24 h. The principle of the mill is similar to that of agitator bead mills in which the grinding media is accelerated with the use of an agitator shaft. The energy supplied to the media is then transferred to the solids via collisions and de-acceleration. The vessel is placed in a horizontal position to allow for even grinding activity and activation. Figure 1 depicts a technical schematic of the Netzsch LME 1 horizontal bead mill. The product inlet and outlet to the grinding chamber were sealed to allow for batch milling. Raw materials and grinding media were added to the vessel through the 'bead filling connection'. At the end of every experimental run, the 'tank floor' or front cap of the milling chamber was removed and the sample and beads collected. The grinding media and mill were washed in preparation for the next experimental run. The pump set-up provided by Netzsch was not used.

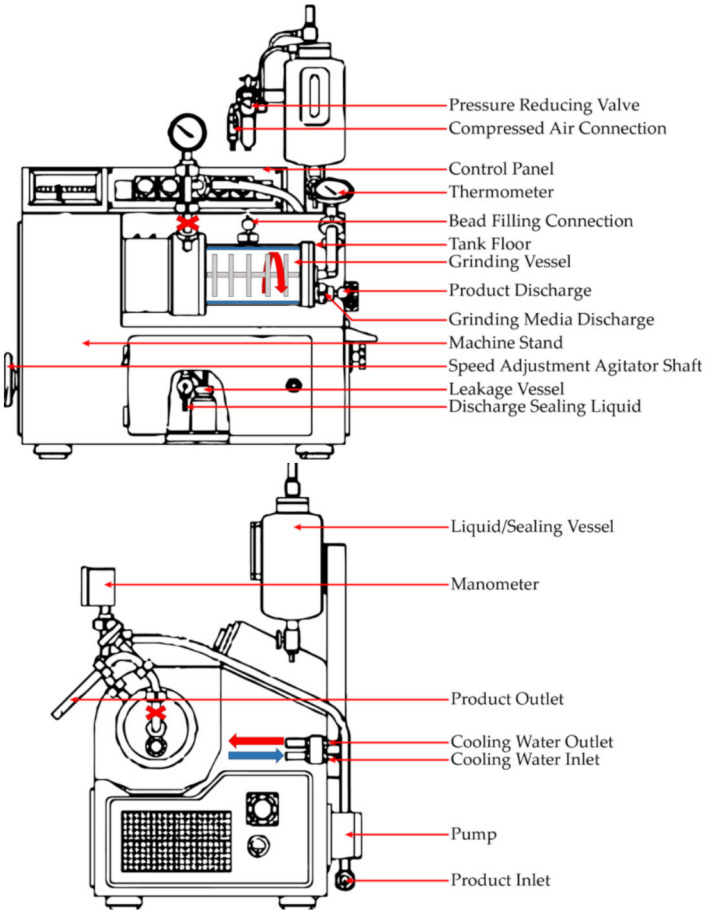

Figure 1. Technical Schematic of Netzsch LME 1 Horizontal Bead Mill as modified from Netzsch.

2.2. *Ageing Process*

The ageing step was conducted by making use of a bench-top Lasec digital hotplate stirrer. Samples obtained from the milling chamber were divided such that half was immediately filtered and dried and the other half subjected to an ageing step. Samples were placed in a glass beaker and agitated, at 400 rpm, for 24 h. Sample temperature was elevated and kept constant at 80 °C. A thin plastic film was placed over the beaker to prevent excessive moisture loss. Experiments were performed without the use of an inert gas under air atmosphere. All samples were filtered and dried at 60 °C for 12 h.

2.3. Mg-Al LDH

Commercial grade MgO (86%, Chamotte Holdings, JHB, GP, ZA) was initially calcined at 800 °C for 1 h to eliminate carbonate and hydroxide contaminants. This was then milled with $Al(OH)_3$ (Hindalco, Belgaum, India) making use of a 2:1 (28.63 g MgO, 23.83 g $Al(OH)_3$) (S1) and 3:1 (33.79 g MgO, 18.75 g $Al(OH)_3$) (S2), M^{II}:M^{III} metal ratio [15,26]. The selected MgO contained SiO_2 as an impurity and was prevalent in all relevant samples collected.

2.4. Ca-Al LDH

Commercial grade $Ca(OH)_2$ (LimeCo. Minerals, JHB, GP, ZA) was first calcined at a temperature of 900 °C for 1 h to remove any hydroxide and carbonate impurities, to form CaO. This was then reacted with 100 mL water for 15 min to form $Ca(OH)_2$. This step eliminated the possibility of vapor formation within the milling chamber due to the extremely exothermic CaO hydration reaction. The $Ca(OH)_2$ and $Al(OH)_3$ (Hindalco, Belgaum, India) were milled with and without the addition of a carbonate source, $CaCO_3$ (Kulubrite 45, Idwala Carbonates, Port Edward, KZN, ZA). The selected metal starting ratios were Ca:Al:$CaCO_3$ of 2:1:0 (35.80 g CaO, 16.60 g $Al(OH)_3$)(S4) and 3:2:1 (25.93 g CaO, 15.91 g $Al(OH)_3$, 10.58 g $CaCO_3$)(S3) [21].

2.5. Zn-Al LDH

The synthesis of Zn-Al LDH was conducted with $Zn_5(CO_3)_2(OH)_6$ (Sigma-Aldridge, St. Louis, MO, USA). This was milled at a 1:1 (Zn:Al) metal ratio with $Al(OH)_3$ (Hindalco, Belgaum, India). The sample was further referred to as S5 (30.69 g $Zn_5(CO_3)_2(OH)_6$, 21.77 g $Al(OH)_3$) [18].

2.6. Cu-Al LDH

Commercial grade $Cu_2(OH)_2CO_3$ (Adchem, MELB, AU) and $Al(OH)_3$ (Hindalco, Belgaum, India) were milled making use of a 2:1 (Cu:Al) ratio with the aim of synthesising $Cu_2Al(OH)_5CO_3{\cdot}XH_2O$ (38.97 g $Cu_2(OH)_2CO_3$, 13.75 g $Al(OH)_3$) (S6) [17].

2.7. Material Characterisation

2.7.1. Particle Size Analysis (PSA)

Samples collected were analysed wet and fully dispersed, before the filtration and drying steps, with the use of a Mastersizer 3000 (Malvern Panalytical, Malvern, UK) using a Hydro LV liquid unit.

2.7.2. Scanning Electron Microscopy (SEM)

SEM imaging was used to observe the morphology of the prepared samples. A Zeiss Gemini 1 cross beam 540 FEG SEM (Oberkochen, Germany). Powdered samples were placed secured onto an aluminium sample holder and graphite coated 5 times with a Polaron Equipment E5400 SEM auto-coating sputter system (Quorum, East Sussex, UK).

2.7.3. X-ray Diffraction Analysis (XRD)

Reaction products of powdered samples were identified using a PANalytical X'Pert Pro powder diffractometer in θ-θ configuration fitted with an X'Celerator detector and variable divergence- and fixed receiving slits (Malvern Panalytical, Malvern, UK). The system made use of Fe filtered Co-Kα (λ = 1.789Å) source. Samples were prepared using the standardised PANalytical backloading system, providing a random distribution of particles. Samples were scanned from 5° to 90° with a step size of 0.008°. Sample mineralogy was determined using the ICSD database in correlation with X'Pert Highscore plus software.

2.7.4. Fourier Transform Infrared Spectroscopy (FT-IR)

FT-IR spectra for the samples were obtained using a PerkinElmer 100 Spectrophotometer (Massachusetts, USA) over a range of 550–4000 cm^{-1} and represent an average of 32 scans, at a resolution of 2 cm^{-1}.

2.7.5. X-ray Fluorescence (XRF)

XRF was used for elemental analysis of the samples. Samples were dried at 100 °C and roasted at 1000 °C to determine mass loss on ignition. In addition, 1 g of the sample was mixed with 6 g Lithumtetraborate flux and fused at 1050 °C to form a stable fused glass bead. Analysis was conducted using a Thermo Fisher ARL Perform 'X Sequential instrument (Massachusetts, USA). Samples were characterised using UNIQUANT software.

3. Results and Discussion

3.1. Particle Size Analysis

The particle size of the raw material mixtures as well as that of the sample obtained is depicted in Tables 1 and 2, respectively. It was noted that overall particle size reduction occurred for most samples, with the exception of S3, with an increase in the grinding time as expected. This could possibly be attributed to the formation and agglomeration of Ca-Al LDH present within the sample. Raw material mixtures exhibited large D_{90} measurements that could be attributed to immediate reaction with water, as well as agglomeration.

Table 1. Particle size analysis of raw material mixtures prior to milling, relevant to each sample.

Sample	D_{10} [μm]	D_{50} [μm]	D_{90} [μm]
S1	2.35	7.79	17.6
S2	1.66	7.22	18.8
S3	1.98	7.84	23.6
S4	2.29	9.17	686
S5	1.71	4.13	10.5
S6	1.34	5.55	15.6

Table 2. Particle size analysis of each sample after 1 h of wet milling in a Netzsch LME 1 horizontal bead mill.

Sample	D_{10} [μm]	D_{50} [μm]	D_{90} [μm]
S1	0.962	3.39	6.21
S2	0.693	2.33	4.94
S3	0.594	1.70	36.9
S4	0.661	2.71	86.0
S5	0.77	2.51	4.83
S6	0.764	2.43	4.93

3.2. X-ray Fluorescence

The elemental composition and metal ratios of the samples were obtained via XRF analysis and listed in Table 3. All samples were found to have a small amount of zirconium, yttrium, and iron contamination from the milling media and the milling chamber. Samples S1 and S2 contained SiO_2 introduced by the selected commercial grade MgO reagent. XRF analysis was conducted to ensure that the correct metal ratios were applied to the raw materials added to the system and are therefore not an indication of the composition of the LDH phases present within each sample. They are an indication of the metal ratios within the overall sample obtained. Calculated metal ratios were observed to correlate with those adapted from literature.

Table 3. Calculated M^{II}:M^{III} ratios of each sample, after wet milling for 1 h with a Netzsch LME 1 horizontal bead mill, as obtained through XRF analysis.

Sample	Expected M^{II}:M^{III} Ratio	Calculated M^{II}:M^{III} Ratio
S1	2.00: 1.00	2.00:1.04
S2	3.00:1.00	3.00:1.04
S3	2.00:1.00	2.00:1.09
S4	2.00:1.00	2.00:0.94
S5	1.00:1.00	1.00:1.01
S6	2.00:1.00	2.00:10.00

3.3. X-ray Diffraction Analysis

Samples analysed were observed to have minor unindexed peaks present. This could be attributed to unidentified phases present or impurities due to mill degradation. Future studies should be conducted in attempt to adequately investigate all phases present within samples obtained.

Mg-Al LDH. Figures 2 and 3 show the XRD spectra obtained for samples S1 and S2. The reaction had not yet reached completion at the selected synthesis conditions prior to ageing. The sample synthesised with a 2:1 metal ratio (S1) exhibited no clear LDH peaks with no crystalline LDH phase detected within the sample. Ageing of the sample resulted in a clear LDH pattern with primary and secondary peaks located at 2θ values of 13.49° and 27.22°, respectively. This correlated with a basal spacing of 0.759 nm. Comparatively, S2 exhibited primary and secondary LDH peaks prior to ageing at 2θ values of 13.37° and 26.99°, respectively. This correlated with a basal spacing of 0.767 nm. Ageing of the sample resulted in more complete conversion of raw materials to LDH product, with clear peaks observed at 2θ values of 13.48° and 27.10°. The basal spacing was calculated to be 0.760 nm. Basal spacing has been found to be influenced by numerous factors including milling time, the amount of water present and possible carbonate contamination [15]. Lattice imperfections as a result of mechanically induced amorphitisation could further contribute to larger basal spacing values [5]. The addition of water has been known to decrease the degree of supersaturation, which could negatively impact morphology and crystallinity of the synthesised LDHs. It has further been observed that the crystallinity of LDHs can pass through a maximum, with lattice imperfections increasing with an increase in milling time [26]. The calculated basal spacing values obtained for both S1 and S2, after ageing, were found to be similar with those reported in literature [15]. Similarly, spectra for the aged samples obtained further correlated with existing literature [9,15,27].

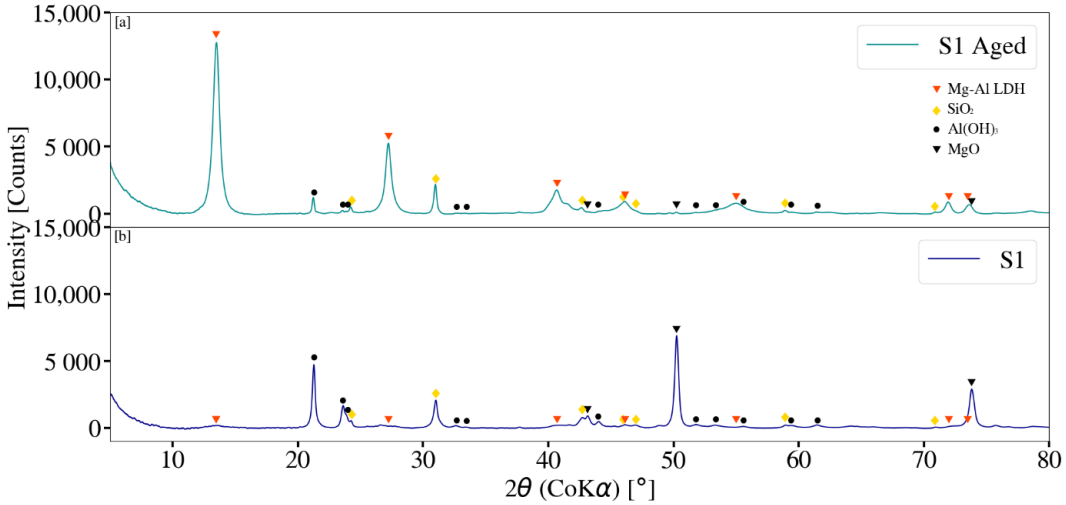

Figure 2. (**a**) X-ray diffraction analysis of the Mg-Al LDH sample (S1), synthesised with a 2:1 M^{II}:M^{III} ratio, after ageing for 24 h at 80 °C.; (**b**) X-ray diffraction analysis of sample S1 prior to ageing after 1 h of wet milling at 2000 rpm.

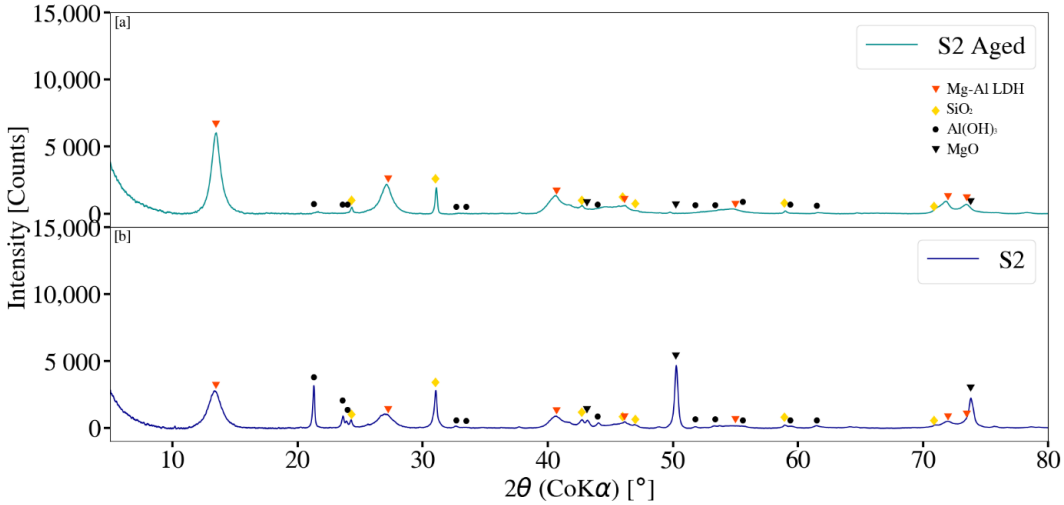

Figure 3. (**a**) X-ray diffraction analysis of Mg-Al LDH sample (S2), synthesised with a 3:1 M^{II}:M^{III} ratio after ageing for 24 h at 80 °C; (**b**) X-ray diffraction analysis of sample S2 prior to ageing after 1 h of wet milling at 2000 rpm.

Ca-Al LDH. XRD reflection patterns for samples S3 and S4 are as depicted in Figures 4 and 5, respectively. The presence of LDH was observed prior to ageing for S3 with a primary peak at a 2θ of 13.50°. This correlated to a basal spacing of 0.759 nm. Ageing of the sample improved conversion of raw materials to LDH product, with a decrease in $Al(OH)_3$ and $Ca(OH)_2$ peak intensity observed. Twinning primary peaks were observed at 2θ values of 13.54° and 13.20° corresponding to basal spacing's of 0.757 nm and 0.776 nm, respectively. Comparatively, the XRD spectra for S4 depicted the presence of LDH within the sample despite the lack of a direct carbonate source. The primary peak was observed to occur at 2θ of 13.47°, with a basal spacing of 0.761 nm. The presence of $CaCO_3$ was further noted and likely due to atmospheric carbonate contamination. Ageing of the sample resulted in the formation of katoite ($Ca_3Al_2(OH)_{12}$) as well as twinning primary LDH peaks. These were observed to occur at 2θ of 13.27° and 13.58°, corresponding to basal spacing of 0.772 nm and 0.755 nm. Twinning peaks could be attributed to the presence of different LDH phases within the sample and differ through carbonate content [22,27,28]. Basal spacing values obtained for both samples, before and after ageing, suggest the presence of either or a mixture of calcium monocarboaluminate and a dehydrated polymorph of calcium hemicarboaluminate that forms upon ageing. Basal spacing reported for each of these were 0.750 nm [22,27] and 0.760–0.770 nm [22,28], respectively. Ca-Al LDH synthesised in the presence of a carbonate source formed more readily when compared to that synthesised with no $CaCO_3$. Previous studies have shown that Ca-Al LDH and katoite (tricalcium aluminate) can result when reacting $Ca(OH)_2$ and $Al(OH)_3$ in the absence of an additional phase or carbonate source, with little to no LDH formation occurring at times [11,21,29]. Studies have also shown that, upon the addition of a third phase such as $CaCO_3$ or $CaCl_2{\cdot}2H_2O$ LDH, formation occurs more readily with little to no katoite formation. This suggests a complex relationship between the formation of Ca-Al LDH and katoite. It has been suggested that the presence of pillared anions such as Cl^- and CO_3^{2-} assist in the formation of the layered structure of Ca-Al LDH. The third phase therefore stabilises the Ca-Al LDH structure allowing for formation to occur more readily [21].

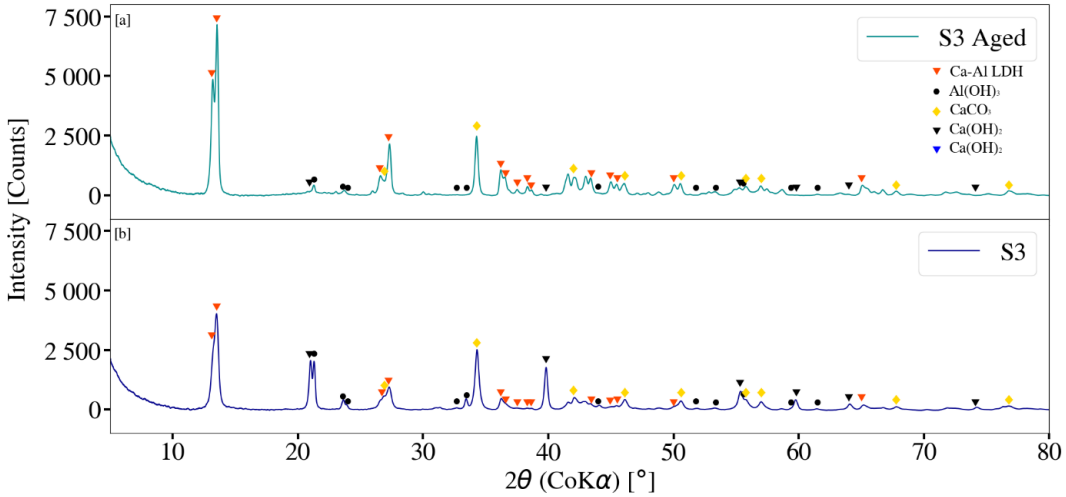

Figure 4. (**a**) X-ray diffraction analysis of sample Ca-Al LDH sample (S3), synthesised with a 2:1 M^{II}:M^{III} ratio, in the presence of a carbonate source, after ageing for 24 h at 80 °C.; (**b**) X-ray diffraction analysis of sample S3 prior to ageing, after 1 h of wet milling at 2000 rpm.

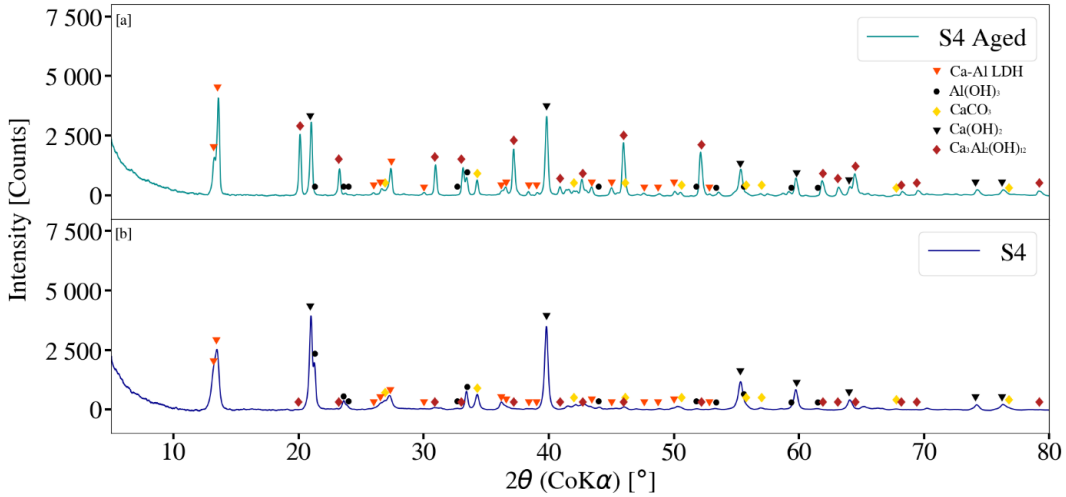

Figure 5. (**a**) X-ray diffraction analysis of sample Ca-Al LDH sample (S4), synthesised with a 2:1 M^{II}:M^{III} ratio, without the presence of a carbonate source, after ageing for 24 h at 80 °C.; (**b**) X-ray diffraction analysis of sample S4 prior to ageing after 1 h of wet milling at 2000 rpm.

Zn-Al LDH. The XRD patterns of samples S5 are depicted in Figure 6. The primary LDH peak was observed to occur at a 2θ value of 13.86°, corresponding to a basal-spacing of 0.749 nm. Conversion prior to ageing was observed to be incomplete with $Zn_5(CO_3)_2(OH)_6$ and $Al(OH)_3$ peaks observed at 2θ values of 15.08° and 21.31°, respectively. Ageing of the sample resulted in the increase in LDH peak intensity with a primary peak at 2θ of 13.70 which corresponds to a basal spacing of 0.748 nm. A decrease in raw material peaks were observed with ageing; however, conversion remained incomplete for the selected synthesis conditions. Metal ratios (M^{II}:M^{III}) typically employed for the synthesis of Zn-Al LDH are between 2:1 and 4:1 for conventional methods such as co-precipitation [18]. It has recently been suggested that molar ratios suitable for mechanochemical synthesis range between 1:1 and 2:1, with nearly pure phase Zn-Al LDH as the result [18]. Slight differences were observed for basal spacing values obtained. These were observed to differ from those reported in literature (0.758 nm, $Zn_4CO_3(OH)_6{\cdot}H_2O$ as starting material) with the Zn content influencing the basal spacing obtained [18].

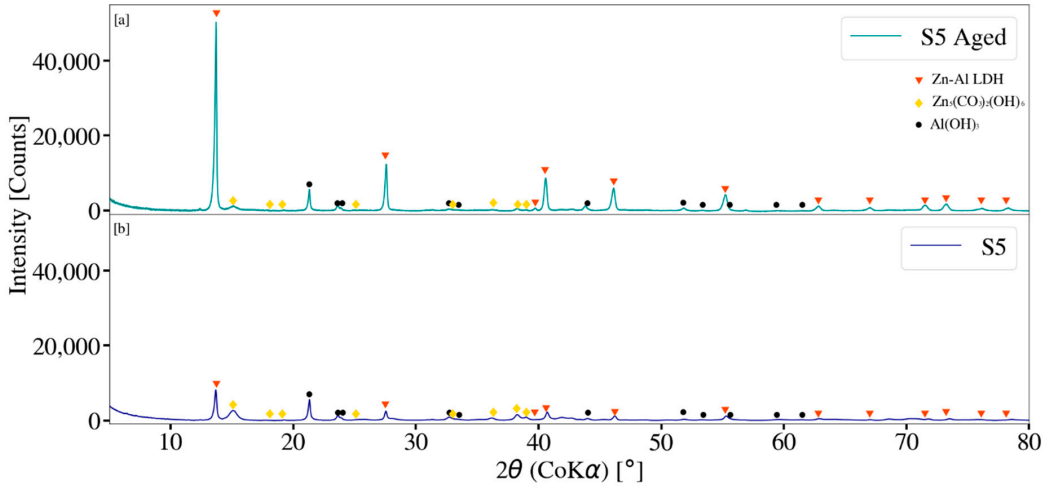

Figure 6. (**a**) X-ray diffraction analysis of Zn-Al LDH sample (S5), synthesised with a 1:1 M^{II}:M^{III} ratio, after ageing for 24 h at 80 °C.; (**b**) X-ray diffraction analysis of sample S5 prior to ageing after 1 h of wet milling at 2000 rpm.

Cu-Al LDH. The XRD spectra obtained for samples S6 and $Cu_2(OH)_2CO_3$ can be seen in Figure 7. The results for S6 prior to ageing were considered to be inconclusive as no obvious LDH peaks were identified. A decrease in $Cu_2(OH)_2CO_3$ peak intensities were, however, observed to occur after 1 h of milling activity. Ageing of the sample resulted in the formation of a peak at 13.74° with a second peak present at approximately 27.76°. Identification of the LDH peaks were difficult due to prominent and overlapping $Cu_2(OH)_2CO_3$ peaks. Basal spacing associated with the observed primary peak was determined to be 0.746 nm. This was observed to be smaller than that reported in literature (0.754 nm) [17]. The formation of Cu-Al LDH was reported to be dependent on the selected rotational speed and therefore the degree of amorphitization [17].

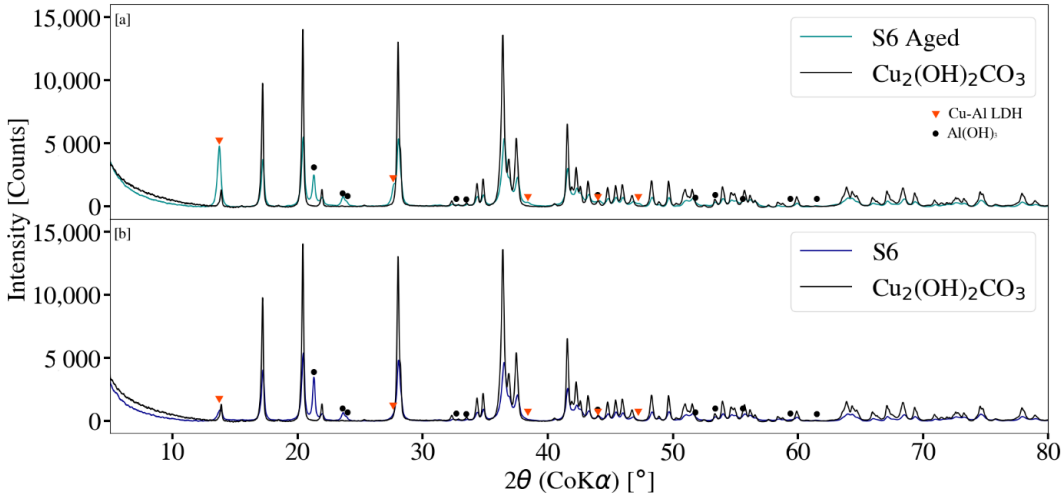

Figure 7. (**a**) X-ray diffraction analysis of Cu-Al LDH sample (S6), synthesised with a 2:1 M^{II}:M^{III} ratio, after ageing for 24 h at 80 °C.; (**b**) X-ray diffraction analysis of sample S6 prior to ageing after 1 h of wet milling at 2000 rpm.

3.4. Fourier Transform Infrared Spectroscopy

The main purpose of the FT-IR data was to support the notion that LDH was present within each sample. This was due to the fact that not all LDH peaks were easily identifiable when conducting XRD analysis.

Mg-Al LDH. The FT-IR spectra for S1 and S2, before and after ageing, are depicted in Figures 8 and 9. Prior to ageing peaks were observed to occur between 3500 cm^{-1} and 3700 cm^{-1} for both samples and could be attributed to the stretching vibrations of free –OH groups [15]. Similarly, peaks located between 3250 cm^{-1} and 3600 cm^{-1} are likely due to bonded –OH within both samples [15]. Peaks located at 1367 cm^{-1} (S1) and 1365 cm^{-1} (S2) could be attributed to carbonate interactions (CO_3^{2-} *v3* vibrations) [9,15,20]Ageing of the samples at 80 °C for 24 h, resulted in the intensification of these peaks. A broad peak, from 3250–3700 cm^{-1}, specifically 3425 cm^{-1} (S1) and 3460 cm^{-1} (S2), was observed to form upon ageing of both samples. This could be assigned to the –OH stretching vibrations that occur within the layered brucite like structure of the LDH as well as interlayer water molecules [9,15,20]. Peaks observed between 500 and 900 cm^{-1} could be attributed to M-O and MO-H (M = Mg, Al) vibrations [30]. Peaks located from 1100–900 cm^{-1} are typical of Si-O interactions from SiO_2 impurities in the MgO raw material [30]. The FT-IR spectra for both S1 and S2 after ageing coincide with spectra observed in literature [9,15,20,27].

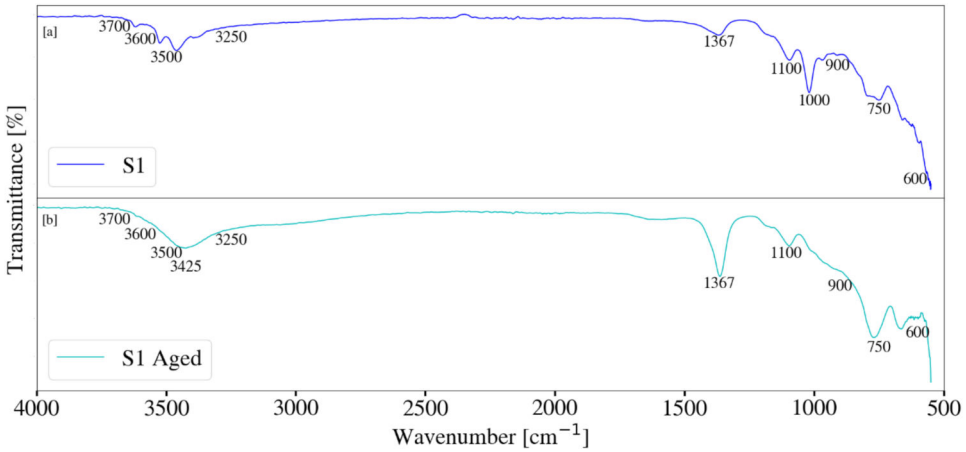

Figure 8. (**a**) FT-IR analysis of the Mg-Al LDH sample (S1) prior to ageing, synthesised with a 2:1 M^{II}:M^{III} ratio, after 1 h of wet milling at 2000 rpm.; (**b**) FT-IR analysis of sample S1 after ageing for 24 h at 80 °C.

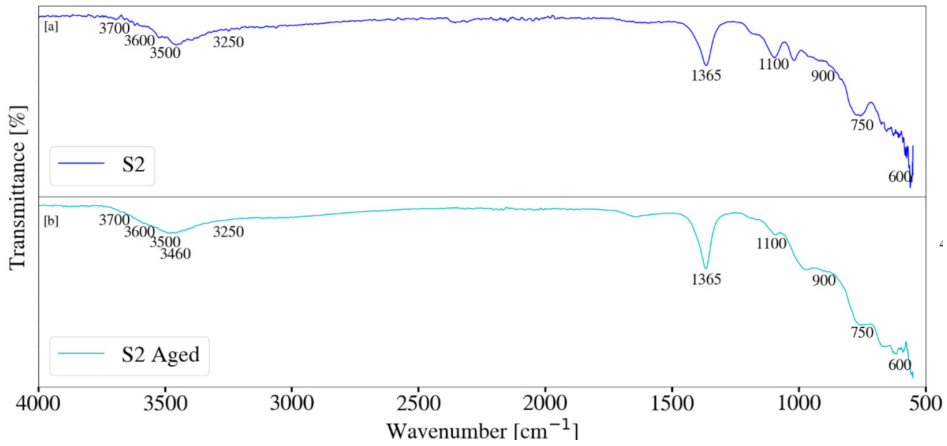

Figure 9. (**a**) FT-IR analysis of the Mg-Al LDH sample (S2) prior to ageing, synthesised with a 3:1 M^{II}:M^{III} ratio, after 1 h of wet milling at 2000 rpm.; (**b**) FT-IR analysis of sample S2 after ageing for 24 h at 80 °C.

Ca-Al LDH. FT-IR spectra for S3 and S4, before and after, ageing are depicted in Figures 10 and 11. Peaks observed between 3700–3300 cm^{-1} could be due to MO-H vibrations within each sample [5,21] as well as the vibration of –OH (*v2*) within the inorganic main layers of the LDH structure [5]. Prior to ageing, S3 depicted peaks at 1418 cm^{-1} and 876 cm^{-1}, which could be due to carbonate vibrations on

the surface of the LDH structure present [5,21]. Similarly peaks at 1370 cm^{-1} could be attributed to CO_3^{2-} *v3* vibrations within the interlayer of the LDH structure [21]. Ageing of the sample resulted in similar spectra to that obtained prior to ageing. The twinning carbonate interactions observed near 1366 cm^{-1} have been suggested further to be the result of two different environments for carbonate present, likely due to different Ca-Al LDH phases present [27]. The spectra for S4 prior to ageing were observed to be similar to that of S3. Peaks observed at 1414 cm^{-1} could be the result of carbonate within the system [5,21]. Synthesis, drying, and ageing were conducted, without the use of an inert gas, under air atmosphere. Carbonate contamination was therefore possible. Ageing of the sample resulted in the formation of twinning peaks at 1366 cm^{-1} and 1415 cm^{-1}. These could once again be attributed to interlayer and surface carbonate interactions of LDH formed within the system [5,21].

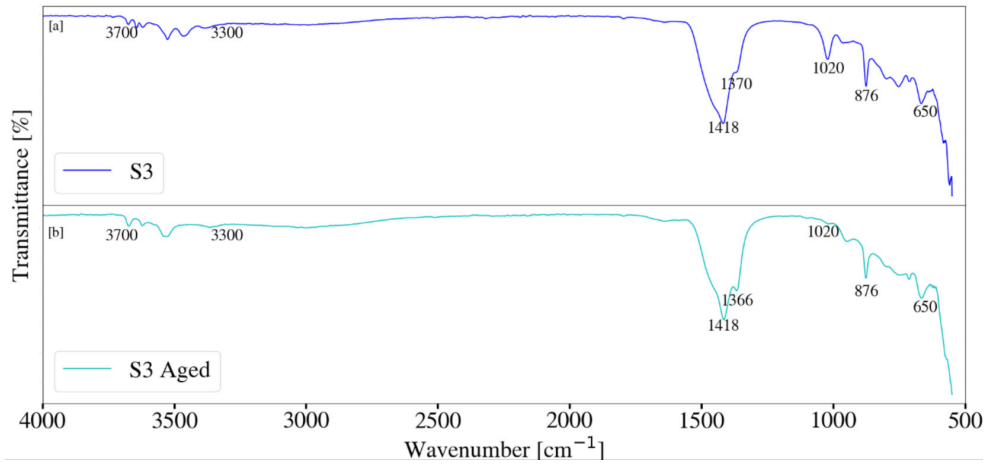

Figure 10. (**a**) FT-IR analysis of the Ca-Al LDH sample (S3) prior to ageing, synthesised with a 2:1 M^{II}:M^{III} ratio in the presence of a Carbonate source, after 1 h of wet milling at 2000 rpm.; (**b**) FT-IR analysis of sample S3 after ageing for 24 h at 80°.

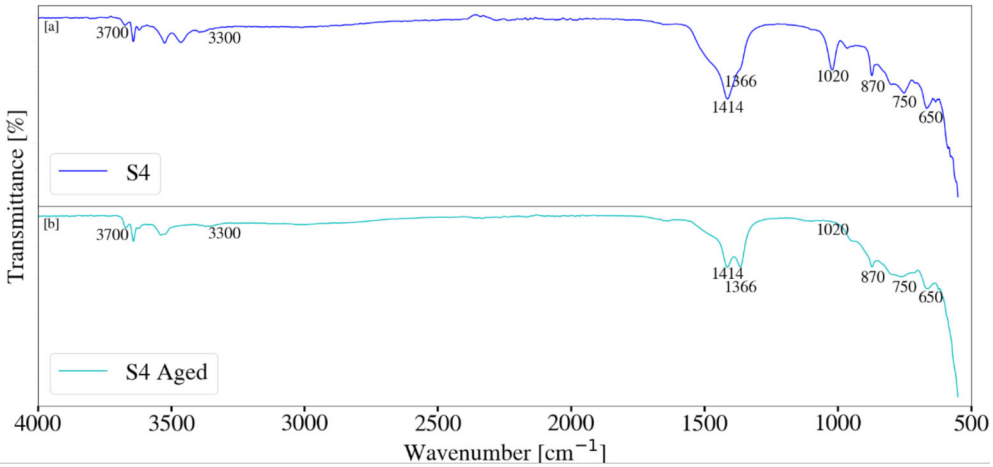

Figure 11. (**a**) FT-IR analysis of the Ca-Al LDH sample (S4) prior to ageing, synthesised with a 2:1 M^{II}:M^{III} ratio in the absence of a Carbonate source, after 1 h of wet milling at 2000 rpm.; (**b**) FT-IR analysis of sample S4 after ageing for 24 h at 80 °C.

Zn-Al LDH. The FT-IR spectra for S5, as well as that of $Zn_5(CO_3)_2(OH)_6$, is depicted in Figure 12. The peaks at and before 3468 cm^{-1} could be attributed to the stretching vibrations of –OH groups within the sample [18]. Spectra of the sample was observed to resemble that of the $Zn_5(CO_3)_2(OH)_6$ raw material before implantation of the ageing step. Ageing of the sample resulted in more complete conversion of raw materials to LDH product. Broadening of peaks between 3000 cm^{-1} and 3700 cm^{-1} were noted and are due to O-H stretching of hydroxyl groups [31]. Peak formation at approximately

1356 cm^1 and 1620 cm^{-1} was observed and is likely due to the asymmetric stretching vibrations of CO_3^{2-} within the interlayer of the LDH [18,30,31]. Peaks below 1000 cm^{-1} could further be attributed to M-O vibrations (M = Zn, Al) [18,31].

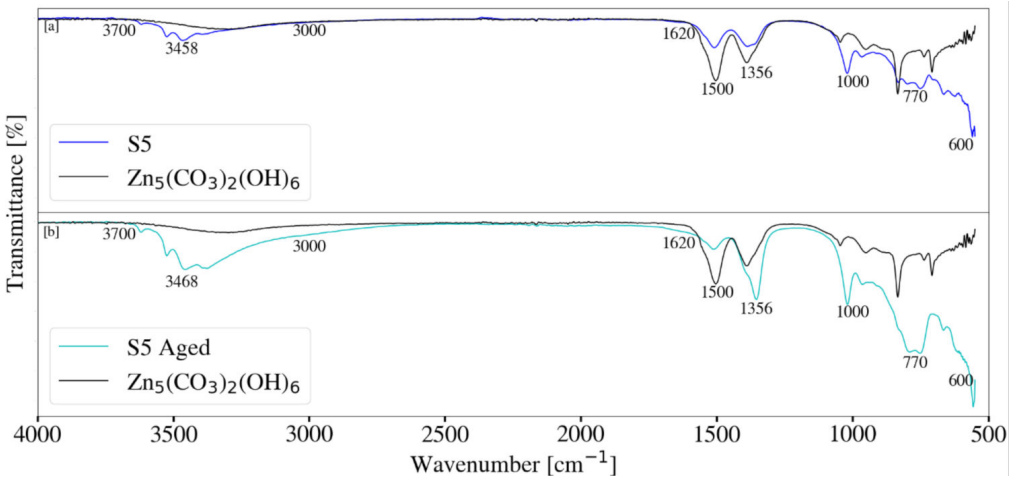

Figure 12. (**a**) FT-IR analysis of the Zn-Al LDH sample (S5) prior to ageing, synthesised with a 1:1 M^{II}:M^{III} ratio, after 1 h of wet milling at 2000 rpm; (**b**) FT-IR analysis of sample S5 after ageing for 24 h at 80 °C.

Cu-Al LDH. The FT-IR spectra for S6 and $Cu_2(OH)_2CO_3$, before and after ageing, are depicted in Figure 13. Samples obtained depicted similar spectra to that of the $Cu_2(OH)_2CO_3$. Identification of bond interactions associated specifically with LDH was therefore difficult and inconclusive. It was noted, however, that additional and broadening of peaks occurred between 3300 cm^{-1} and 3700 cm^{-1} and was consistent with Cu-Al LDH spectra reported in literature [17,32]. Additional peaks could further be attributed to bonded and free –OH groups within the sample [30]. Ageing resulted in the formation of a minor peak at 1632 cm^{-1} which could be due to the vibrations of water molecules [17].

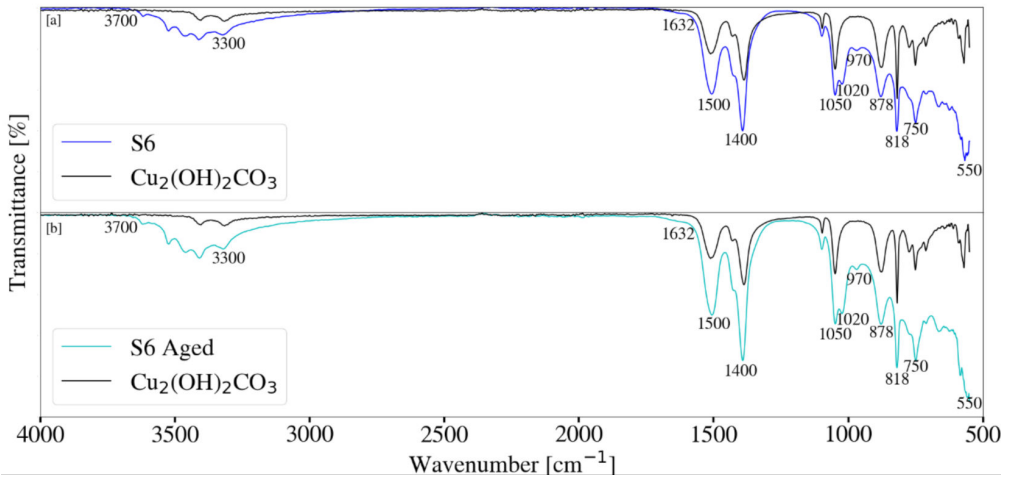

Figure 13. (**a**) FT-IR analysis of the Cu-Al LDH sample (S6) prior to ageing, synthesised with a 2:1 M^{II}:M^{III} ratio, after 1 h of wet milling at 2000 rpm.; (**b**) FT-IR analysis of sample S6 after ageing for 24 h at 80 °C.

3.5. Scanning Electron Microscopy

SEM imaging was conducted to provide insight on the morphology of the samples obtained before and after ageing and is depicted in Figure 14. Prior to ageing, both S1 and S2 depicted similar morphology with no obvious differences observed. Ageing of the samples resulted in the formation of

thin platelet like structures. These were observed to correlate with SEM images associated with Mg-Al LDH reported in literature [9]. No obvious morphological differences were observed between S3 and S4 prior to ageing. Ageing of S3 resulted in the formation of thin crystalline platelets which correlate to those reported in literature for Ca-Al LDH[1]. Comparatively, S4 depicted structures associated with katoite, calcite, and Ca-Al LDH, and was observed to coincide with the XRD data obtained. No clear morphological differences were observed for S5 and S6 before and after ageing. Platelet like structures could be construed as being present.

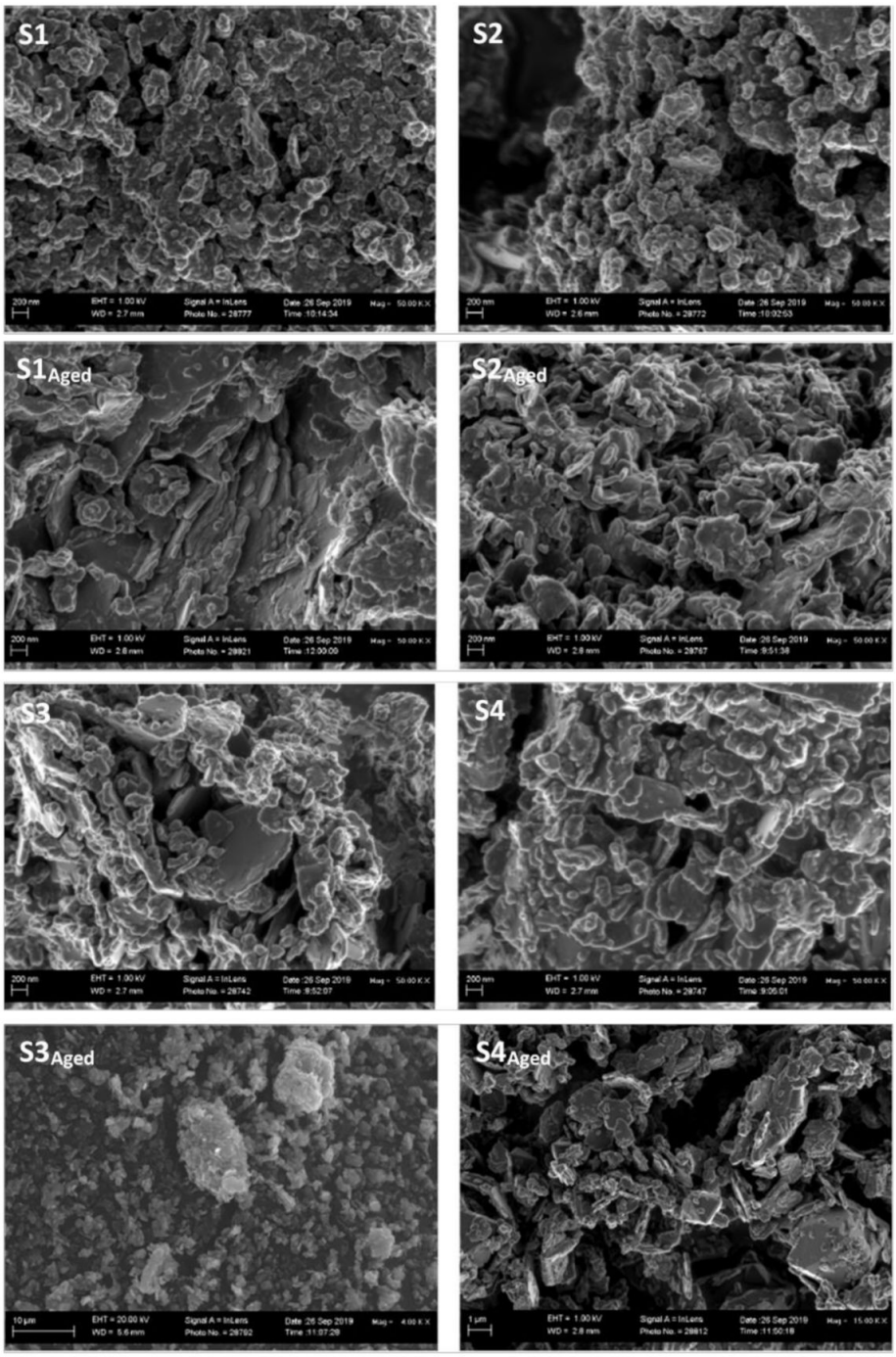

Figure 14. *Cont.*

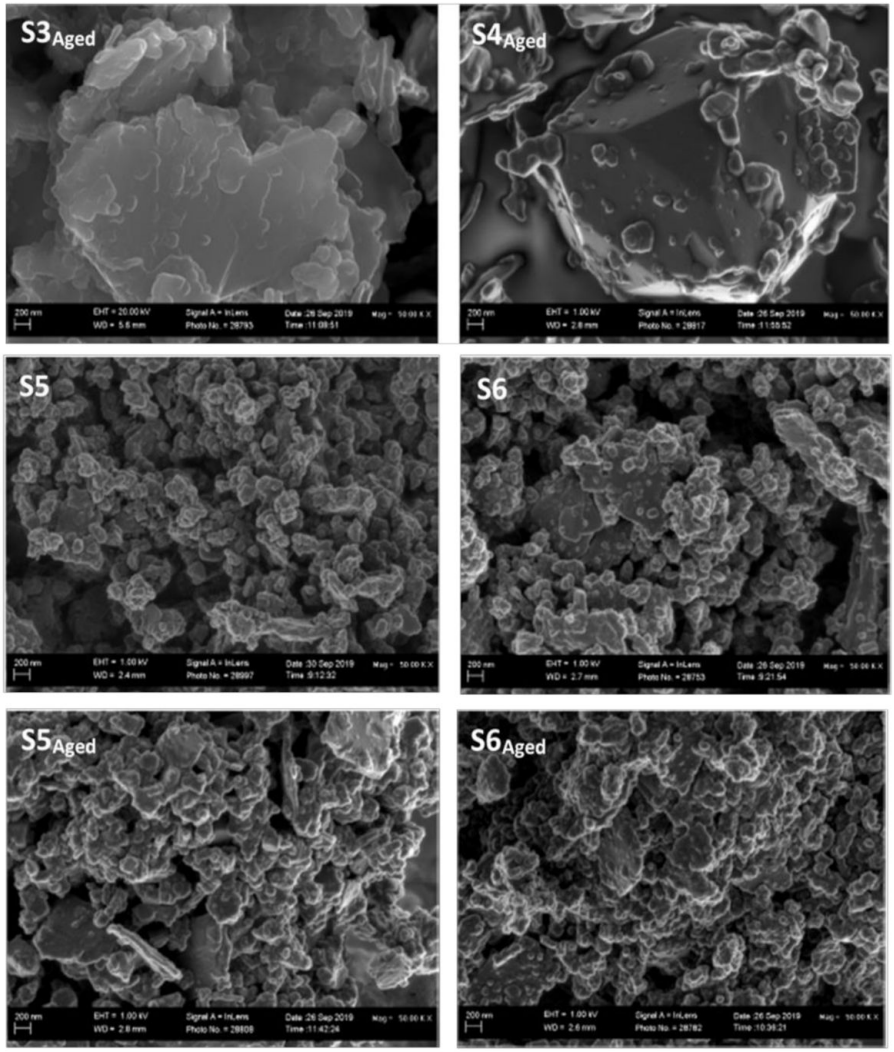

Figure 14. SEM imaging of samples before and after ageing. Imaging was conducted at a magnification of 50.00 K with a 200 nm scale and EHT of 1.00 kV for all samples. Additional imaging was conducted for $S3_{aged}$ at a scale of 10 μm, EHT of 20.00 kV and magnification of 4.00 K. Similarly $S4_{aged}$ was imaged with a scale of 1.00 μm, EHT 1.00 kV and magnification of 15.00 K.

4. Conclusions

A facile mechanochemical method for the synthesis of Mg-Al, Ca-Al, Zn-Al, and Cu-Al LDH was successfully developed. Implementation of ageing resulted in more complete conversion of raw materials to LDH product. Starting materials selected were a mixture of oxides, hydroxides, and basic carbonates, promoting 'green' synthesis of LDH materials. The synthesis method eliminates the use of pH control and avoids the production of salt rich effluent. The selected mill offers potential for commercial up-scaling with a variety of iso mills available, capable of processing large volumes of liquid reagent. Mill operation is versatile offering the potential for batch, semi-batch, or continuous synthesis of LDH materials. Traditional methods have predominantly made use of ball mills, mixer mills, or a mortar and pestle [2]. Wet milling allows for ease of transfer of reagents to downstream processes with little to no process interruption. Inclusion of the ageing step has allowed for an increase in conversion of raw materials to LDH product and improved sample morphology. This offers potential for converting the one-step wet mechanochemical route to that including a second step. Previous studies conducted have indicated that a grinding step is necessary for LDH formation to occur more readily [9,17,18]. The grinding activity allows for mechanochemical activation of raw materials, creating active sites. The selected horizontal bead mill has successfully resulted in the

formation of multiple types of LDH product; however, raw material peaks were still observably present under the selected synthesis conditions. Samples S1, S2, S3, and S5 resulted in successful LDH formation with high intensity peaks observed after ageing. Samples S4 resulted in LDH formation prior to ageing; however, katoite formation occurred during the ageing step. The presence of a carbonate source was therefore necessary for LDH formation to occur and continue successfully. Cu-Al LDH did not form readily, with no clear indication of its presence prior to ageing. LDH peaks were observed to have formed upon ageing with precursor materials still notably present. The mill therefore offers potential for a successful one-step wet mechanochemical technique. Further investigation of a change in milling parameters such as retention time, jacket water temperature, bead size, solids loading and bead loading is warranted.

Author Contributions: B.A.B.: Methodology, Formal Analysis, Investigation, Data Curation, Writing—Original Draft and Final Version, Visualization, Conceptualisation. F.J.W.J.L.: Supervision, Project administration, Funding Acquisition, Writing—Review and Editing, Resources, Conceptualisation, Moral support. All authors have read and agreed to the published version of the manuscript.

Funding: This research project was funded by TeckSparks Pty Ltd. and THRIP.

Conflicts of Interest: The authors declare no conflict of interest.

References

1. Bergaya, F.; Lagaly, G. *Handbook of Clay Science*, 1st ed.; Elsevier Science & Technology Books: San Diego, CA, USA, 2013; pp. 1021–1069.
2. Qu, J.; Zhang, Q.; Li, X.; He, X.; Song, S. Mechanochemical approaches to synthesize layered double hydroxides: A review. *Appl. Clay Sci.* **2015**, *119*, 185–192. [CrossRef]
3. Ferencz, Z.; Szanados, M.; Adok-Sipiczki, M.; Kukovecz, A.; Konya, Z.; Sipos, P.; Palinko, I. Mechanochemical assisted synthesis of pristine Ca(II)Sn(IV)-layered double hydroxides and their amino acid intercalated composites. *Mater. Sci.* **2014**, *49*, 8479–8486. [CrossRef]
4. Li, Z.; Zhang, Q.; Liu, X.; Chen, M.; Wu, L.; Ai, Z. Mechanochemical synthesis of novel heterostructured Bi_2S_3/Zn-Al layered double hydroxide nano-particles as efficient visible light reactive Z-scheme photocatalysts. *Appl. Surf. Sci.* **2018**, *452*, 123–133. [CrossRef]
5. Fahami, A.; Beall, G.W.; Enayatpour, S.; Tavangarian, T.; Fahami, M. Rapid preparation of nano hexagonal-shaped hydrocalumite via one-pot mechanochemistry method. *Appl. Clay Sci.* **2017**, *136*, 90–95. [CrossRef]
6. Fahmi, A.; Duraia, E.M.; Beall, G.W.; Fahami, M. Facile synthesis and structural insight of chloride intercalated Ca-Al Layered double hydroxide nanopowders. *J. Alloys Compd.* **2017**, *727*, 970–977. [CrossRef]
7. Du, W.; Zheng, L.; Li, X.; Fu, J.; Lu, X.; Hou, Z. Plate like Ni-Mg-Al layered double hydroxides synthesised via a solvent free approach and its application in hydrogenolysis of D sorbitol. *App. Clay Sci.* **2016**, *123*, 166–172. [CrossRef]
8. Qu, J.; Li, X.; Lei, Z.; Li, Z.; Chen, M.; Zhang, Q. Mechano-Hydrothermal synthesis of tetraborate pillared Li-Al layered double hydroxide. Am. *Ceram. Soc.* **2016**, *99*, 1151–1154. [CrossRef]
9. Zhang, F.; Du, N.; Song, S.; Liu, J.; Hou, W. Mechano-hydrothermal synthesis of Mg_2Al-NO_3 layered double hydroxides. *Solid State Chem.* **2013**, *206*, 45–50. [CrossRef]
10. Zhang, F.; Hou, W. Mechano-hydrothermal preparation of Li-Al-OH layered double hydroxides. *Sol. State Sci.* **2018**, *79*, 93–98. [CrossRef]
11. Ferencz, Z.; Kukovecz, A.; Konya, A.; Sipos, P.; Palinko, I. Optimisation of the synthesis parameters of mechanochemically prepared Ca-Al-layered double hydroxide. *Appl. Clay Sci.* **2015**, *112*, 94–99. [CrossRef]
12. Kuramoto, K.; Intasa-ard, S.; Bureekaew, S.; Ogawa, M. Mechanochemical synthesis of finite particles of layered double hydroxide-acetate intercalation compound: Swelling, Thin film ion exchange. *Sol. State Chem.* **2017**, *253*, 147. [CrossRef]
13. Tongamp, W.; Zhang, Q.; Saito, F. Mechanochemical route for synthesizing nitrate form layered double hydroxide. *Powder Technol.* **2008**, *185*, 43–48. [CrossRef]
14. Pagano, C.; Marmottini, F.; Nocchetti, M.; Ramella, D.; Perioli, L. Effects of different milling techniques on the layered double hydroxides final properties. *Appl. Clay Sci.* **2018**, *151*, 124–133. [CrossRef]

15. Tongamp, W.; Zhang, Q.; Saito, F. Preparation of meixnerite (Mg–Al–OH) type layered double hydroxide by a mechanochemical route. *Mater. Sci.* **2007**, *42*, 9210–9215. [CrossRef]
16. Li, Z.; Chen, M.; Ai, Z.; Wu, L.; Zhang, Q. Mechanochemical synthesis of CdS/MgAl LDH-precursor as improved visible light driven photocatalyst for organic dye. *App. Clay Sci.* **2018**, *163*, 265–272. [CrossRef]
17. Qu, J.; He, X.; Chen, M.; Hu, H.; Zhang, Q.; Liu, X. Mechanochemical synthesis of Cu-Al and methyl orange intercalated Cu-Al layered double hydroxides. *Mater. Chem. Phys.* **2017**, *191*, 173–180. [CrossRef]
18. Qu, J.; He, X.; Chen, M.; Huang, P.; Zhang, Q.; Liu, X. A facile mechanochemical approach to synthesize Zn-Al layered double hydroxide. *Solid State Chem.* **2017**, *250*, 1–5. [CrossRef]
19. Zhong, L.; He, X.; Qu, J.; Li, X.; Lei, Z.; Zhang, Q.; Liu, X. Precursor preparation for Ca-Al layered double hydroxide to remove hexavalent chromium co-existing with calcium and magnesium chloride. *Solid State Chem.* **2017**, *245*, 200–206. [CrossRef]
20. Fahami, A.; Beall, G.W. Mechanosynthesis and characterization of Hydrotalcite like Mg–Al–SO4-LDH. *Mater. Lett.* **2016**, *165*, 192–195.
21. Qu, J.; Zhong, L.; Li, Z.; Chen, M.; Zhang, Q.; Liu, X. Effect of anion addition on the syntheses of Ca–Al layered double hydroxide via a two-step mechanochemical process. *Appl. Clay Sci.* **2016**, *124*, 267–270. [CrossRef]
22. Szabados, M.; Mészáros, R.; Erdei, S.; Kónya, Z.; Kukovecz, Á.; Sipos, P.; Pálinkó, I. Ultrasonically enhanced mechanochemical synthesis of Ca-Al-layered double hydroxides intercalated by a variety of inorganic anions. *Ultrason. Sonochem.* **2016**, *31*, 409–416. [CrossRef] [PubMed]
23. Szabados, M.; Pásztor, K.; Csendes, Z.; Muráth, S.; Kónya, Z.; Kukovecz, Á.; Carlson, S.; Sipos, P.; Pálinkó, I. Synthesis of high-quality, well-characterised CaAlFe layered triple hydroxide with the combination of dry-milling and ultrasonic irradiation in aqueous solution at elevated temperature. *Ultrason. Sonochem.* **2016**, *32*, 173–180. [CrossRef] [PubMed]
24. Szabados, M.; Varga, G.; Kónya, Z.; Kukovecz, Á.; Carlson, S.; Sipos, P.; Pálinkó, I. Ultrasonically-enhanced preparation, characterization of Ca-Fe-layered double hydroxides with various interlayer halide, azide and oxo anions (CO_3^{2-},NO_3^-,ClO_4^-). *Ultrason. Sonochem.* **2018**, *40*, 853–860. [CrossRef]
25. Iwasaki, T.; Yoshii, H.; Nakamura, H.; Watano, S. Simple and rapid synthesis of Ni-Fe Layered double hydroxide by a new mechanochemical method. *Appl. Clay Sci.* **2012**, *58*, 120–124. [CrossRef]
26. Zhang, X.; Qi, F.; Li, S.; Wei, S.; Zhou, K. A mechanochemical approach to get stunningly uniform magnesium aluminium layered double hydroxides. *Appl. Surf. Sci.* **2012**, *259*, 245–251. [CrossRef]
27. Labuschagne, F.J.W.J.; Molefe, D.M.; Focke, W.W.; van der Westhuizen, I.; Wright, H.C.; Royeppen, M.D. Heat stabilising flexible PVC with layered double hydroxide derivatives. *Polym. Degrad.* **2015**, *113*, 49–54. [CrossRef]
28. Rosenberg, S.P.; Wilson, D.J.; Heath, C.A. Some Aspects of Calcium Chemistry in the Bayer Process. *Light Met.* **2001**, *1*, 210–216.
29. Kano, J.; Yamashita, J.; Saito, F. Effect of heat-assisted grinding of calcium hydroxide-gibbsite mixture on formation of hydrated calcium aluminate and its hydration behavior. *Powder Technol.* **1998**, *98*, 279–280. [CrossRef]
30. Socrates, G. *Infrared and Ramen Characteristic Group Frequencies: Tables and Charts*, 1st ed.; John Wiley and Sons: Hoboken, NJ, USA, 2001; pp. 287–295.
31. Qu, J.; He, X.; Li, X.; Ai, Z.; Li, Y.; Zhang, Q.; Liu, X. Precursor preparation of Zn–Al layered double hydroxide by ball milling for enhancing adsorption and photocatalytic decoloration of methyl orange. *RSC Adv.* **2017**, *7*, 31466–31474. [CrossRef]
32. Qu, J.; He, Z.; Lei, Q.; Zhang, Q.; Liu, X. Mechanochemical synthesis of dodecyl sulfate anion intercalated Cu-Al layered double hydroxide. *Solid State Sci.* **2017**, *74*, 125–130. [CrossRef]